Inorganic Chemistry

Article

pubs.acs.org/IC

Effect of the Piperazine Unit and Metal-Binding Site Position on the Solubility and Anti-Proliferative Activity of Ruthenium(II)- and Osmium(II)- Arene Complexes of Isomeric Indolo[3,2-*c*]quinoline—Piperazine Hybrids

Lukas K. Filak,[†,‡] Danuta S. Kalinowski,*[,§] Theresa J. Bauer,[†] Des R. Richardson,*[,§] and Vladimir B. Arion*[,†]

[†]Institute of Inorganic Chemistry, University of Vienna, Währinger Strasse 42, A-1090 Vienna, Austria

[‡]School of Chemical Sciences, The University of Auckland, Private Bag 92019, Auckland 1142, New Zealand

[§]Molecular Pharmacology and Pathology Program, Department of Pathology and Bosch Institute, The University of Sydney, Sydney, New South Wales 2006, Australia

Supporting Information

ABSTRACT: In this study, the indoloquinoline backbone and piperazine were combined to prepare indoloquinoline—piperazine hybrids and their ruthenium- and osmium-arene complexes in an effort to generate novel antitumor agents with improved aqueous solubility. In addition, the position of the metal-binding unit was varied, and the effect of these structural alterations on the aqueous solubility and antiproliferative activity of their ruthenium- and osmium-arene complexes was studied. The indoloquinoline—piperazine hybrids L^{1-3} were prepared *in situ* and isolated as six ruthenium and osmium complexes $[(\eta^6\text{-}p\text{-cymene})M(L^{1-3})Cl]Cl$, where L^1 = 6-(4-methylpiperazin-1-yl)-*N*-(pyridin-2-yl-methylene)-11*H*-indolo-[3,2-*c*]quinolin-2-*N*-amine, M = Ru ([**1a**]Cl), Os ([**1b**]Cl), L^2 = 6-(4-methylpiperazin-1-yl)-*N*-(pyridin-2-yl-methylene)-11*H*-indolo[3,2-*c*]quinolin-4-*N*-amine, M = Ru ([**2a**]Cl), Os ([**2b**]Cl), L^3 = 6-(4-methylpiperazin-1-yl)-*N*-(pyridin-2-yl-methylene)-11*H*-indolo[3,2-*c*]quinolin-8-*N*-amine, M = Ru ([**3a**]Cl), Os ([**3b**]Cl). The compounds were characterized by elemental analysis, one- and two-dimensional NMR spectroscopy, ESI mass spectrometry, IR and UV—vis spectroscopy, and single-crystal X-ray diffraction. The antiproliferative activity of the isomeric ruthenium and osmium complexes [**1a,b**]Cl—[**3a,b**]Cl was examined *in vitro* and showed the importance of the position of the metal-binding site for their cytotoxicity. Those complexes containing the metal-binding site located at the position 4 of the indoloquinoline scaffold ([**2a**]Cl and [**2b**]Cl) demonstrated the most potent antiproliferative activity. The results provide important insight into the structure—activity relationships of ruthenium- and osmium-arene complexes with indoloquinoline—piperazine hybrid ligands. These studies can be further utilized for the design and development of more potent chemotherapeutic agents.

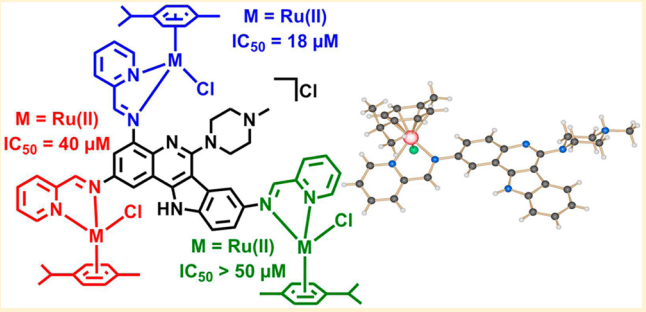

INTRODUCTION

The search for more effective ruthenium complexes and organoruthenium compounds as chemotherapeutic agents with fewer side effects than currently clinically applied platinum compounds continues to attract attention.[1−8] In fact, the use of biologically active ligands in combination with ruthenium is an option to achieve synergistic effects.[9] The effect of metal coordination on their antiproliferative activity, alteration of their pharmacological properties, is an area of study that requires further investigation.

Paullones or indolo[3,2-*d*]benzazepines (Figure 1, top left and top middle), initially predicted to exhibit a cyclin-dependent kinase (CDK) inhibitory profile similar to that of flavopiridol,[10,11] were later shown to act as protein kinase inhibitors,[12,13] targeting glycogen synthase kinase-3β and mitochondrial malate dehydrogenase.[14,15] However, their clinical use was hampered by their limited aqueous solubility. One way to potentially overcome this problem was the coordination of these organic compounds to metal ions. Complexes with gallium(III),[16,17] ruthenium,[18] copper(II),[19] as well as organoruthenium(II) and organoosmium(II) compounds have been synthesized, and due to their improved aqueous solubility, their antiproliferative activity has been investigated.[20−24] In fact, interesting structure—activity relationships have been established. For example, replacement of the seven-membered azepine ring in modified paullones by a six-membered pyridine ring has led to another class of biologically

Received: April 8, 2014
Published: June 13, 2014

   dx.doi.org/10.1021/ic500825j | *Inorg. Chem.* 2014, 53, 6934−6943

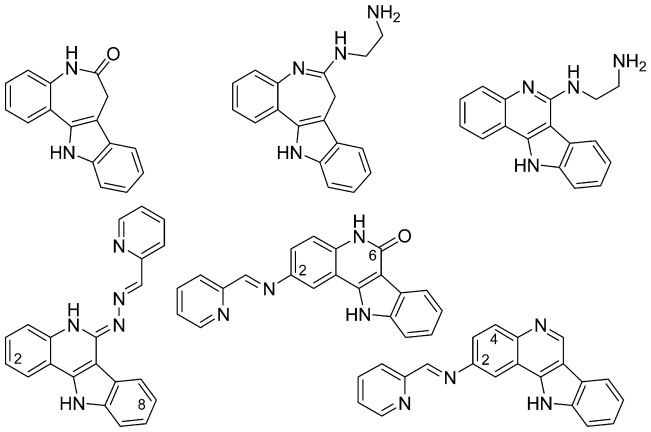

Figure 1. Original paullone, also named indolo[3,2-*d*]benzazepin-6-one (top left),[11] modified paullone (top middle),[23] and modified indolo[3,2-*c*]quinolines with specific atom positions labeled (top right and bottom)[27−29] as ligands for ruthenium(II) and osmium(II).

active compounds, namely, indolo[3,2-*c*]quinolines (Figure 1, top right and bottom).

Although specific kinase inhibition has not been documented for indolo[3,2-*c*]quinolines,[25] tree extracts containing indolo-[3,2-*b*] and indolo[3,2-*c*]quinolines have a long history of usage in traditional African medicine.[26] The main difference compared to the paullones is the full conjugation of the heterocyclic system, leading to the planarity of the indoloquinoline backbone. This resulted in different physicochemical properties and a marked alteration in the biological activity of these indoloquinolines.[23] It was discovered that the modified paullones containing an ethylenediamine binding moiety (Figure 1, top middle) formed ruthenium- and osmium-arene complexes that were more stable compared to their indoloquinoline counterparts[23] (Figure 1, top right). However, the complexes with indoloquinolines were approximately 1 order of magnitude more cytotoxic.[23]

Interestingly, replacement of the sp^3-hybridized nitrogen donor atoms with sp^2-hybridized nitrogens present in the formylpyridine−azine modified indoloquinolines (Figure 1, bottom left) afforded complexes that do not dissociate with liberation of the indoloquinoline ligand under biological conditions.[27,28] These studies enabled elucidation of the effects of substituents at positions 2 and 8 of the indoloquinoline backbone (Figure 1, bottom left) on their biological activity.[27,28]

Further structural diversity was achieved through synthetic procedures involving the reduction of a nitro group at position 2 of the indoloquinoline backbone. This created a potential metal-binding site via condensation of the emerging NH_2 group with 2-formylpyridine. This, in combination with the preservation of the lactam group, resulted in a new class of paullone analogues (Figure 1, bottom middle).[29] This group was of particular interest since the lactam group of the metal-free paullones was shown to be essential for efficient CDK inhibition.[11] Their resulting ruthenium and osmium indoloquinoline complexes exhibited lower *in vitro* antiproliferative activity.[29] In fact, their efficacy was 2 orders of magnitude lower when compared to complexes with ligands coordinated via a similar binding site at position 6 of the backbone.[29] Furthermore, one osmium complex with the ligand shown in Figure 1 (bottom right) demonstrated antitumor activity *in vivo*.[29] Intriguingly, this complex showed activity not only after intraperitoneal injection, but also when administered orally.[29]

We were interested in combining bioactive substructures, namely, that of the indoloquinoline backbone with a piperazine heterocycle, to improve the water solubility of the indoloquinoline moiety. Moreover, piperazine is frequently found in the structures of biologically active compounds in a large spectrum of therapeutic areas.[30−33] Some of these agents, such as Ciprofloxacin, Ofloxacin, Posaconazole, Enoxacin, Eperezolid, and Piperacillin, are currently used successfully in clinical therapy.[34−36] Metal-based derivatives of biologically active compounds containing this heterocyclic nucleus as a pharmacophore have been also reported.[37−41] An efficient approach to the synthesis of water-soluble biologically active compounds is the attachment of piperazine or a modified piperazine heterocycle to lipophilic pharmacophore moieties.[42−44] Further modulation of hydrophilic/lipophilic balance can be achieved by introducing different substituents to the distant N atom on the piperazine ring.[45]

Furthermore, it was also of interest to vary the metal-binding unit position and to study the effect of these changes on the aqueous solubility and antiproliferative activity of the ruthenium- and osmium-arene complexes.

Herein, we report the *in situ* synthesis and characterization of three isomeric indoloquinoline−methyl-piperazine conjugates with the location of the metal-binding site at position 2, 4, or 8 of the indoloquinoline scaffold. These compounds were isolated as six water-soluble ruthenium- or osmium-arene complexes of the general formulas $[(\eta^6\text{-}p\text{-cymene})M(L^{1-3})Cl]^+$

Chart 1. Ruthenium- and Osmium-Arene Complexes with Indoloquinoline−Piperazine Hybrid Ligands Modified at Position 2, 4 or 8

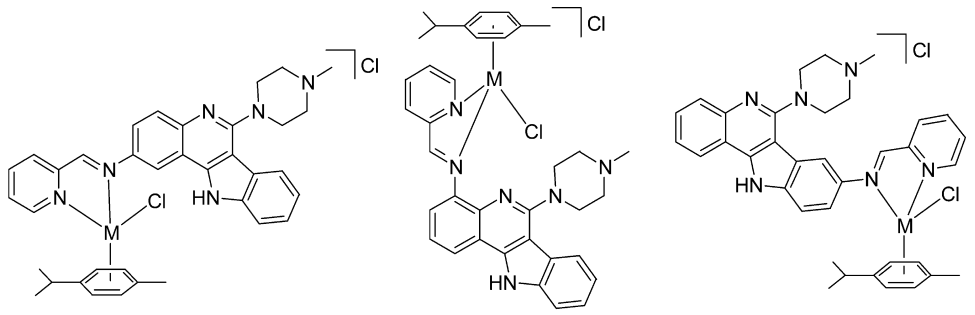

[**1a**]Cl: M = Ru(II)
[**1b**]Cl: M = Os(II)

[**2a**]Cl: M = Ru(II)
[**2b**]Cl: M = Os(II)

[**3a**]Cl: M = Ru(II)
[**3b**]Cl: M = Os(II)

dx.doi.org/10.1021/ic500825j | *Inorg. Chem.* 2014, 53, 6934−6943

(Chart 1). The effects of the metal-binding unit position and the identity of the metal (Ru vs Os) on the antiproliferative activity of isomeric ruthenium- and osmium-arene complexes with indoloquinoline−piperazine hybrids have been elucidated. The results obtained provide an important insight into the structure−activity relationships of ruthenium- and osmium-arene complexes with indoloquinoline−piperazine hybrids and can be utilized further for the design and development of more effective chemotherapeutic agents.

EXPERIMENTAL SECTION

Materials. 2-Aminobenzylamine, phosphorus oxychloride, 1-methylpiperazine, and iron powder were purchased from Sigma-Aldrich (St. Louis, MO), while isatin, 5-nitroisatin, and 2-pyridinecarboxaldehyde were purchased from Acros (Geel, Belgium). All chemicals, as well as the synthesized precursors, were used without further purification. 2-Amino-5-nitrobenzylamine hydrochloride was synthesized according to a procedure published elsewhere.[46] The free amine was obtained by the dissolution of the hydrochloride in a minimal amount of water, addition of 4 equiv of aqueous ammonia, and collection of the formed precipitate by filtration. Ethanol was dried over molecular sieves (3 Å), and tetrahydrofuran (THF) was dried by using a standard procedure (Na/benzophenone).[47]

General Synthetic Procedure (A) for the Synthesis of Complexes [1b]Cl, [2b]Cl, and [3a,b]Cl. The corresponding 2-, 4-, or 8-amino-6-(4-methylpiperazin-1-yl)-indolo[3,2-*c*]quinoline (1 equiv) and the respective metal-*p*-cymene dimer, $[RuCl(\mu\text{-}Cl)(\eta^6\text{-}p\text{-cymene})]_2$ or $[OsCl(\mu\text{-}Cl)(\eta^6\text{-}p\text{-cymene})]_2$ (0.9 equiv), were suspended in dry ethanol. 2-Pyridinecarboxaldehyde (0.9 equiv) was added, and the reaction mixture was stirred under an argon atmosphere, whereupon a clear solution was obtained within a few minutes. After stirring at room temperature for 20 h, the solution was filtered through a GF-3 fiber filter and then added dropwise into dried diethyl ether over sodium sulfate (approximately 400 mL of diethyl ether per 3 mL of solution). The precipitate formed was filtered off and dried *in vacuo* at 45 °C.

(η^6-*p*-Cymene)[6-(4-methylpiperazin-1-yl)-κ*N*-(pyridin-2-yl-methylene)-11*H*-indolo[3,2-*c*]quinolin-2-κ*N*-amine]-chloridoruthenium(II) Chloride, [1a]Cl. 2-Amino-6-(4-methylpiperazin-1-yl)-indolo[3,2-*c*]quinoline (50 mg, 0.15 mmol) and $[RuCl(\mu\text{-}Cl)(\eta^6\text{-}p\text{-cymene})]_2$ (0.04 g, 0.07 mmol) were suspended in deionized water (1 mL) in a Schlenk tube. 2-Pyridinecarboxaldehyde (13 μL, 0.14 mmol) was added, and the resulting suspension was stirred under an argon atmosphere at room temperature for 24 h. The resulting precipitate was filtered off and dried *in vacuo* at 45 °C. Yield: 45 mg, 41%. Anal. Calcd for $C_{36}H_{38}Cl_2N_6Ru\cdot3.75H_2O$ (M_r = 794.26), %: C, 54.44; H, 5.77; N, 10.58. Found, %: C, 54.35; H, 5.54; N, 10.57. Solubility in sodium phosphate buffer (20 mM, pH 7.40): ≥ 6.4 mg/mL. ^{1}H NMR (500 MHz, deuterated dimethyl sulfoxide (DMSO-d_6)): 13.18 (s, 1H, H^{11}), 9.66 (d, 1H, ^3J = 5.4 Hz, H^{15}), 9.20 (s, 1H, H^{13}), 8.80 (s, 1H, H^1), 8.41−8.34 (m, 2H, H^{17} + H^{18}), 8.09−8.05 (m, 2H, H^3 + H^4), 8.01 (d, 1H, ^3J = 8.0 Hz, H^7), 7.96−7.92 (m, 1H, H^{16}), 7.80 (d, 1H, ^3J = 8.0 Hz, H^{10}), 7.55−7.51 (m, 1H, H^9), 7.45−7.40 (m, 1H, H^8), 6.20 (d, 1H, ^3J = 6.2 Hz, $H^{cy2}/H^{cy2\prime}$), 5.90 (d, 1H, ^3J = 6.2 Hz, $H^{cy1}/H^{cy1\prime}$), 5.72 (d, 1H, ^3J = 6.2 Hz, $H^{cy2}/H^{cy2\prime}$), 5.69 (d, 1H, ^3J = 6.2 Hz, $H^{cy1}/H^{cy1\prime}$), 3.60 (br s, 4H, CH_2^{mp}), 2.81 (br s, 4H, CH_2^{mp}), ∼2.50 (m, 1H, H^{cy3}, overlapped with DMSO signal), 2.42 (br s, 3H, CH_3^{mp}), 2.25 (s, 3H, H^{cy5}), 1.01−0.96 (m, 6H, H^{cy4}). ^{13}C NMR (125 MHz, DMSO-d_6): 167.40 (CH, C^{13}), 158.46 (C_q, C^6), 156.73 (CH, C^{15}), 155.03 (C_q, C^{13a}), 147.53 (C_q, C^2), 145.39 (C_q, C^{4a}), 142.64 (C_q, C^{11a}), 140.62 (CH, C^{17}), 139.14 (C_q, C^{10a}), 130.39 (CH, C^{18}), 129.45 (CH, C^{16}), 129.32 (CH, C^4), 125.53 (CH, C^9), 124.16 (CH, C^3), 122.19 (CH, C^7), 121.46 (CH, C^8), 121.44 (C_q, C^{6b}), 115.71 (C_q, C^{11b}), 115.20 (CH, C^1), 112.52 (CH, C^{10}), 107.02 (C_q, C^{6a}), 105.42 (C_q, C^{cy2a}), 104.56 (C_q, C^{cy1a}), 87.43 (CH, $C^{cy2}/C^{cy2\prime}$), 87.10 (CH, $C^{cy2}/C^{cy2\prime}$), 85.74 (CH, $C^{cy1}/C^{cy1\prime}$), 85.25 (CH, $C^{cy1}/C^{cy1\prime}$), 55.0 (CH_2, CH_2^{mp}), 49.3 (CH_2, CH_2^{mp}), 46.2 (CH_3, CH_3^{mp}), 31.01 (CH, C^{cy3}), 22.24 (CH_3, $C^{cy4}/C^{cy4\prime}$), 22.16 (CH_3, $C^{cy4}/C^{cy4\prime}$), 18.93 (CH_3, C^{cy5}) ppm.

(η^6-*p*-Cymene)[6-(4-methylpiperazin-1-yl)-κ*N*-(pyridin-2-yl-methylene)-11*H*-indolo[3,2-*c*]quinolin-2-κ*N*-amine]-chloridoosmium(II) Chloride, [1b]Cl. The compound was synthesized by following the general synthetic procedure (A) starting from 2-amino-6-(4-methylpiperazin-1-yl)-indolo[3,2-*c*]quinoline (0.15 g, 0.45 mmol), $[OsCl(\mu\text{-}Cl)(\eta^6\text{-}p\text{-cymene})]_2$ (0.16 g, 0.20 mmol) and 2-pyridinecarboxaldehyde (39 μL, 0.41 mmol) in dry ethanol (3 mL). Yield: 178 mg, 52%. Anal. Calcd for $C_{36}H_{38}Cl_2N_6Os\cdot1.5H_2O$ (M_r = 842.89), %: C, 51.30; H, 4.90; N, 9.97. Found, %: C, 51.43; H, 4.97; N, 9.87. Solubility in sodium phosphate buffer (20 mM, pH 7.40): ≥ 8.4 mg/mL. ^{1}H NMR (500 MHz, DMSO-d_6): 13.15 (s, 1H, H^{11}), 9.62−9.59 (m, 2H, H^{13} + H^{15}), 8.73 (s, 1H, H^1), 8.52 (d, 1H, ^3J = 7.6 Hz, H^{18}), 8.36−8.31 (m, 1H, H^{17}), 8.05 (d, 1H, ^3J = 8.8 Hz, H^4), 8.01 (d, 1H, ^3J = 8.1 Hz, H^7), 7.97 (dd, 1H, ^3J = 8.8 Hz, ^4J = 2.4 Hz H^3), 7.92−7.88 (m, 1H, H^{16}), 7.79 (d, 1H, ^3J = 8.0 Hz, H^{10}), 7.55−7.51 (m, 1H, H^9), 7.45−7.40 (m, 1H, H^8), 6.48 (d, 1H, ^3J = 5.8 Hz, $H^{cy2}/H^{cy2\prime}$), 6.11 (d, 1H, ^3J = 5.8 Hz, $H^{cy1}/H^{cy1\prime}$), 5.92 (d, 1H, ^3J = 5.8 Hz, $H^{cy2}/H^{cy2\prime}$), 5.84 (d, 1H, ^3J = 5.8 Hz, $H^{cy1}/H^{cy1\prime}$), 3.58 (br s, 4H, CH_2^{mp}), 2.76 (s, 4H, CH_2^{mp}), 2.44−2.36 (m, 4H, H^{cy3} + CH_3^{mp}), 2.33 (br s, 3H, H^{cy5}), 0.94−0.92 (m, 6H, H^{cy4} + $H^{cy4\prime}$). ^{13}C NMR (125 MHz, DMSO-d_6): 168.23 (CH, C^{13}), 158.59 (C_q, C^6), 156.49 (C_q, C^{13a}), 156.42 (CH, C^{15}), 147.52 (C_q, C^2), 145.52 (C_q, C^{4a}), 142.58 (C_q, C^{11a}), 140.77 (CH, C^{17}), 139.12 (C_q, C^{10a}), 130.29 (CH, C^{16}), 130.20 (CH, C^{18}), 129.30 (CH, C^4), 125.52 (CH, C^9), 124.54 (CH, C^3), 122.20 (CH, C^7), 121.47 (CH, C^8), 121.44 (C_q, C^{6b}), 115.72 (CH, C^1), 115.63 (C_q, C^{11b}), 112.51 (CH, C^{10}), 107.01 (C_q, C^{6a}), 98.55 (C_q, C^{cy1a}), 97.19 (C_q, C^{cy2a}), 79.66 (CH, $C^{cy2}/C^{cy2\prime}$), 79.24 (CH, $C^{cy2}/C^{cy2\prime}$), 76.40 (CH, $C^{cy1}/C^{cy1\prime}$), 75.75 (CH, $C^{cy1}/C^{cy1\prime}$), 55.12 (CH_2, CH_2^{mp}), 49.49 (CH_2, CH_2^{mp}), 31.25 (CH, C^{cy3}), 22.60 (CH_3, $C^{cy4}/C^{cy4\prime}$), 22.33 (CH_3, $C^{cy4}/C^{cy4\prime}$), 18.89 (CH_3, C^{cy5}) ppm, CH_3^{mp} not observed.

(η^6-*p*-Cymene)[6-(4-methylpiperazin-1-yl)-κ*N*-(pyridin-2-yl-methylene)-11*H*-indolo[3,2-*c*]quinolin-4-κ*N*-amine]-chloridoruthenium(II) Chloride, [2a]Cl. 4-Amino-6-(4-methylpiperazin-1-yl)-indolo[3,2-*c*]quinoline (0.14 g, 0.43 mmol) and $[RuCl(\mu\text{-}Cl)(\eta^6\text{-}p\text{-cymene})]_2$ (0.12 g, 0.19 mmol) were suspended in deionized water (2.5 mL) in a Schlenk tube. 2-Pyridinecarboxaldehyde (37 μL, 0.39 mmol) was added, and the resulting suspension was stirred under an argon atmosphere at room temperature for 24 h. The resulting precipitate was filtered off and dried *in vacuo*. Yield: 45 mg, 41%. Anal. Calcd for $C_{36}H_{38}Cl_2N_6Ru\cdot2.5H_2O$ (M_r = 771.74), %: C, 56.03; H, 5.62; N, 10.89. Found, %: C, 56.12; H, 5.61; N, 10.87. Solubility in sodium phosphate buffer (20 mM, pH 7.40): ≥ 6.4 mg/mL. ^{1}H NMR (500 MHz, DMSO-d_6): 13.27 (s, 1H, H^{11}), 9.70 (d, 1H, ^3J = 5.5 Hz, H^{15}), 9.34 (s, 1H, H^{13}), 8.66 (d, 1H, ^3J = 8.6 Hz, H^1), 8.42 (d, 1H, ^3J = 7.5 Hz, H^{18}), 8.40−8.36 (m, 1H, H^{17}), 8.29 (d, 1H, ^3J = 7.6 Hz, H^3), 7.99 (d, 1H, ^3J = 8.0 Hz, H^7), 7.97−7.93 (m, 1H, H^{16}), 7.81 (d, 1H, ^3J = 8.1 Hz, H^{10}), 7.76−7.71 (m, 1H, H^2), 7.57−7.52 (m, 1H, H^9), 7.45−7.41 (m, 1H, H^8), 6.15 (d, 1H, ^3J = 6.1 Hz, H^{cy2}), 5.74 (d, 1H, ^3J = 6.1 Hz, H^{cy1}), 5.50−5.47 (m, 2H, $H^{cy1\prime}$ + $H^{cy2\prime}$), 3.55−3.30 (br s, 4H, CH_2^{mp}, in part overlapped with H_2O signal), 2.80−2.60 (br s, 4H, CH_2^{mp}), 2.50−2.42 (m, 1H, H^{cy3}), 2.45−2.25 (br s, 3H, CH_3^{mp}), 2.21 (s, 3H, H^{cy5}), 0.98 (d, 3H, H^{cy4}), 0.93 (d, 3H, $H^{cy4\prime}$). ^{13}C NMR (125 MHz, DMSO-d_6): 172.34 (CH, C^{13}), 156.74 (CH, C^{15}), 155.39 (C_q, C^{13a}), 147.00 (C_q, C^4), 142.72 (C_q, C^{11a}), 140.78 (CH, C^{17}), 139.35 (C_q, C^{10a}), 135.30 (C_q, C^{4a}), 130.17 (CH, C^{18}), 129.46 (CH, C^{16}), 125.67 (CH, C^9), 124.45 (CH, C^3), 123.48 (CH, C^1), 123.28 (CH, C^2), 122.05 (CH, C^7), 121.60 (CH, C^8), 121.26 (C_q, C^{6b}), 117.20 (C_q, C^{11b}), 112.64 (CH, C^{10}), 106.84 (C_q, C^{6a}), 105.38 (C_q, C^{cy2a}), 104.5 (C_q, C^{cy1a}), 87.10 (CH, C^{cy2}), 86.4 (CH, $C^{cy2\prime}$), 85.7 (CH, $C^{cy1\prime}$), 85.01 (CH, C^{cy1}), 48.9 (CH_2, CH_2^{mp}), 30.99 (CH, CH_2^{cy3}), 22.42 (CH_3, $C^{cy4}/C^{cy4\prime}$), 22.35 (CH_3, $C^{cy4}/C^{cy4\prime}$), 19.10 (CH_3, C^{cy5}) ppm, C^6, one CH_2^{mp} and CH_3^{mp} not observed.

(η^6-*p*-Cymene)[6-(4-methylpiperazin-1-yl)-κ*N*-(pyridin-2-yl-methylene)-11*H*-indolo[3,2-*c*]quinolin-4-κ*N*-amine]-chloridoosmium(II) Chloride, [2b]Cl. The compound was synthesized by following the general synthetic procedure (A) starting from 4-amino-6-(4-methylpiperazin-1-yl)-indolo[3,2-*c*]quinoline (0.15 g, 0.45 mmol), $[OsCl(\mu\text{-}Cl)(\eta^6\text{-}p\text{-cymene})]_2$ (0.16 g, 0.20 mmol), and 2-pyridinecarboxaldehyde (39 μL, 0.41 mmol) in dry ethanol (3 mL). Yield: 156 mg, 45%. Anal. Calcd for $C_{36}H_{38}Cl_2N_6Os\cdot1.75H_2O$ (M_r =

dx.doi.org/10.1021/ic500825j | Inorg. Chem. 2014, 53, 6934−6943

Table 1. Crystal Data and Details of Data Collection for $[1aH]Cl_2 \cdot EtOH \cdot 2H_2O$, $[2aH]Cl_2 \cdot 1.5^iPrOH \cdot 0.5H_2O$, and $[2a]Cl \cdot 0.5EtOH \cdot H_2O$

compound	$[1aH]Cl_2 \cdot EtOH \cdot 2H_2O$	$[2aH]Cl_2 \cdot 1.5^iPrOH \cdot 0.5H_2O$	$[2a]Cl \cdot 0.5EtOH \cdot H_2O$
empirical formula	$C_{38}H_{49}Cl_3N_6O_3Ru$	$C_{40.5}H_{52}Cl_3N_6O_2Ru$	$C_{37}H_{43}Cl_2N_6O_{1.5}Ru$
fw	845.25	862.30	767.74
space group	$P2_1/n$	$P2_1/c$	Pc
α, Å	19.2712(14)	15.2896(5)	10.0291(4)
b, Å	7.8687(5)	19.5424(6)	9.4460(4)
c, Å	25.5459(19)	15.3917(5)	19.2958(7)
β, deg	91.724(4)	113.677(2)	93.479(2)
V [Å^3]	3872.0(5)	4211.8(2)	1824.62(13)
Z	4	4	2
λ [Å]	0.710 73	0.710 73	0.710 73
ρ_{calcd}, g cm^{-3}	1.450	1.360	1.397
cryst size, mm^3	0.12 × 0.08 × 0.02	0.25 × 0.13 × 0.03	0.15 × 0.10 × 0.04
T [K]	150(2)	100(2)	100(2)
μ, mm^{-1}	0.657	0.604	0.615
R_1[a]	0.0519	0.0480	0.0362
wR_2[b]	0.1137	0.1422	0.0922
GOF[c]	1.084	1.058	1.036

[a] $R_1 = \Sigma||F_0| - |F_c||/\Sigma|F_0|$. [b] $wR_2 = \{\Sigma[w(F_0^2 - F_c^2)^2]/\Sigma[w(F_0^2)^2]\}^{1/2}$. [c] GOF = $\{\Sigma[w(F_0^2 - F_c^2)^2]/(n - p)\}^{1/2}$, where n is the number of reflections and p is the total number of parameters refined.

847.39), %: C, 51.03; H, 4.94; N, 9.92. Found, %: C, 50.98; H, 4.94; N, 9.88. Solubility in sodium phosphate buffer (20 mM, pH 7.40): ≥ 7.0 mg/mL. ^{1}H NMR (500 MHz, DMSO-d_6): 13.23 (s, 1H, H^{11}), 9.76 (s, 1H, H^{13}), 9.64 (d, 1H, ^3J = 5.6 Hz, H^{15}), 8.64 (d, 1H, ^3J = 7.4 Hz, H^1), 8.56 (d, 1H, ^3J = 7.6 Hz, H^{18}), 8.38−8.33 (m, 1H, H^{17}), 8.15 (d, 1H, ^3J = 7.5 Hz, H^3), 7.99 (d, 1H, ^3J = 8.0 Hz, H^7), 7.93−7.89 (m, 1H, H^{16}), 7.81 (d, 1H, ^3J = 8.1 Hz, H^{10}), 7.75−7.70 (m, 1H, H^2), 7.58−7.52 (m, 1H, H^9), 7.45−7.41 (m, 1H, H^8), 6.45 (d, 1H, ^3J = 5.6 Hz, H^{cy2}), 5.95 (d, 1H, ^3J = 5.6 Hz, H^{cy1}), 5.69 (d, 1H, ^3J = 5.6 Hz, $H^{cy2\prime}$), 5.64 (d, 1H, ^3J = 5.6 Hz, $H^{cy1\prime}$), 3.60−3.20 (br s, 4H, CH_2^{mp}, in part overlapped with H_2O signal), 2.80−2.40 (br s, 4H, CH_2^{mp}, in part overlapped with DMSO signal), 2.38−2.20 (m, 7H, H^{cy3} + CH_3^{mp} + H^{cy5}), 0.91 (d, 3H, ^3J = 6.7 Hz, H^{cy4}), 0.87 (d, 3H, ^3J = 6.7 Hz, $H^{cy4\prime}$). ^{13}C NMR (125 MHz, DMSO-d_6): 172.90 (CH, C^{13}), 156.87 (C_q, C^{13a}), 156.40 (CH, C^{15}), 147.01 (C_q, C^4), 142.69 (C_q, C^{11a}), 140.93 (CH, C^{17}), 139.35 (C_q, C^{10a}), 135.34 (C_q, C^{4a}), 130.32 (CH, C^{16}), 130.01 (CH, C^{18}), 125.69 (CH, C^9), 124.86 (CH, C^3), 123.67 (CH, C^1), 123.11 (CH, C^2), 122.05 (CH, C^7), 121.62 (CH, C^8), 121.26 (C_q, C^{6b}), 117.16 (C_q, C^{11b}), 112.64 (CH, C^{10}), 106.86 (C_q, C^{6a}), 98.4 (C_q, C^{cy1a}), 97.25 (C_q, C^{cy2a}), 79.1 (CH, C^{cy2}), 78.4 (CH, $C^{cy2\prime}$), 76.04 (CH, $C^{cy1\prime}$), 75.3 (CH, C^{cy1}), 55.2 (CH_2, CH_2^{mp}), 49.0 (CH_2, CH_2^{mp}), 45.0 (CH_3, CH_3^{mp}), 31.26 (CH, C^{cy3}), 22.85 (CH_3, C^{cy4}), 22.52 (CH_3, $C^{cy4\prime}$), 19.07 (CH_3, C^{cy5}) ppm, C^6 not observed.

(η^6-*p*-Cymene)[6-(4-methylpiperazin-1-yl)-κN-(pyridin-2-ylmethylene)-11*H*-indolo[3,2-*c*]quinolin-8-κN-amine]chloridoruthenium(II) Chloride, [3a]Cl. The compound was synthesized by following the general synthetic procedure (A) starting from 8-amino-6-(4-methylpiperazin-1-yl)-indolo[3,2-*c*]quinoline (0.15 g, 0.45 mmol), $[RuCl(\mu\text{-}Cl)(\eta^6\text{-}p\text{-cymene})]_2$ (0.13 g, 0.20 mmol), and 2-pyridinecarboxaldehyde (39 μL, 0.41 mmol) in dry ethanol (3 mL). Yield: 189 mg, 60%. Anal. Calcd for $C_{36}H_{38}Cl_2N_6Ru \cdot 2.5H_2O$ (M_r = 771.74), %: C, 56.03; H, 5.62; N, 10.89. Found, %: C, 56.09; H, 5.49; N, 11.04. Solubility in sodium phosphate buffer (20 mM, pH 7.40): ≥ 5.6 mg/mL. ^{1}H NMR (500 MHz, DMSO-d_6): 13.37 (s, 1H, H^{11}), 9.62 (d, 1H, ^3J = 5.6 Hz, H^{15}), 9.10 (s, 1H, H^{13}), 8.52 (d, 1H, ^3J = 7.9 Hz, H^1), 8.37−8.34 (m, 2H, H^{17} + H^{18}), 8.29 (s, 1H, H^7), 7.95−7.89 (m, 4H, H^4 + H^9 + H^{10} + H^{16}), 7.71−7.67 (m, 1H, H^3), 7.57−7.53 (m, 1H, H^2), 6.15 (d, 1H, ^3J = 6.2 Hz, H^{cy2}), 5.81 (d, 1H, ^3J = 6.2 Hz, H^{cy1}), 5.62 (d, 1H, ^3J = 6.1 Hz, $H^{cy2\prime}$), 5.44 (d, 1H, ^3J = 6.1 Hz, $H^{cy1\prime}$), 3.71 (br s, 2H, CH_2^{mp}), 3.49 (br s, 2H, CH_2^{mp}), 2.86 (br s, 4H, CH_2^{mp}), 2.64 (br s, 2H, CH_2^{mp}), 2.56−2.48 (m, 1H, H^{cy3}, overlapped in part with DMSO signal), 2.43−2.27 (br s, 3H, CH_3^{mp}), 2.26 (s, 3H, H^{cy5}), 1.00 (d, 3H, ^3J = 6.9 Hz, H^{cy4}), 0.97 (d, 3H, ^3J = 6.9 Hz, $H^{cy4\prime}$). ^{13}C NMR (125 MHz, DMSO-d_6): 167.25 (CH, C^{13}), 156.51 (CH, C^{15}), 155.31 (C_q, C^{13a}), 146.40 (C_q, C^8), 145.41 (C_q, C^{4a}), 144.21 (C_q, C^{11a}), 140.47 (CH, C^{17}), 139.39 (C_q, C^{10a}), 130.16 (CH, C^{18}), 129.38 (CH, C^3), 129.15 (CH, C^{16}), 128.26 (CH, C^4), 124.20 (CH, C^2), 122.49 (CH, C^1), 121.72 (C_q, C^{6b}), 120.14 (CH, C^9), 115.97 (C_q, C^{11b}), 115.58 (CH, C^7), 112.86 (CH, C^{10}), 106.68 (C_q, C^{6a}), 104.86 (2 C_q, C^{cy1a} + C^{cy2a}), 87.58 (CH, C^{cy2}), 87.11 (CH, $C^{cy2\prime}$), 85.19 (CH, C^{cy1}), 84.99 (CH, $C^{cy1\prime}$), 54.8 (CH_2, CH_2^{mp}), 49.8 (CH_2, CH_2^{mp}), 46.0 (CH_3, CH_3^{mp}), 30.98 (CH, C^{cy3}), 22.37 (CH_3, C^{cy4}), 21.93 (CH_3, $C^{cy4\prime}$), 19.04 (CH_3, C^{cy5}) ppm, C^6 not observed.

(η^6-*p*-Cymene)[6-(4-methylpiperazin-1-yl)-κN-(pyridin-2-ylmethylene)-11*H*-indolo[3,2-*c*]quinolin-8-κN-amine]chloridoosmium(II) Chloride, [3b]Cl. The compound was synthesized by following the general synthetic procedure (A) starting from 8-amino-6-(4-methylpiperazin-1-yl)-indolo[3,2-*c*]quinoline (0.15 g, 0.45 mmol), $[OsCl(\mu\text{-}Cl)(\eta^6\text{-}p\text{-cymene})]_2$ (0.16 g, 0.20 mmol), and 2-pyridinecarboxaldehyde (39 μL, 0.41 mmol) in dry ethanol (3 mL). Yield: 204 mg, 58%. Anal. Calcd for $C_{36}H_{38}Cl_2N_6Os \cdot 2.25H_2O$ (M_r = 856.40), %: C, 50.49; H, 5.00; N, 9.81. Found, %: C, 50.49; H, 4.93; N, 9.99. Solubility in sodium phosphate buffer (20 mM, pH 7.40): ≥ 6.8 mg/mL. ^{1}H NMR (500 MHz, DMSO-d_6): 13.44 (s, 1H, H^{11}), 9.57 (d, 1H, ^3J = 5.6 Hz, H^{15}), 9.51 (s, 1H, H^{13}), 8.54 (d, 1H, ^3J = 7.9 Hz, H^1), 8.48 (d, 1H, ^3J = 7.7 Hz, H^{18}), 8.34−8.29 (m, 1H, H^{17}), 8.21 (s, 1H, H^7), 7.94−7.89 (m, 2H, H^{10} + H^4), 7.89−7.83 (m, 2H, H^9 + H^{16}), 7.72−7.67 (m, 1H, H^3), 7.56−7.53 (m, 1H, H^2), 6.44 (d, 1H, ^3J = 5.7 Hz, H^{cy2}), 6.03 (d, 1H, ^3J = 5.7 Hz, H^{cy1}), 5.81 (d, 1H, ^3J = 5.6 Hz, $H^{cy2\prime}$), 5.60 (d, 1H, ^3J = 5.6 Hz, $H^{cy1\prime}$), 3.70 (br s, 2H, CH_2^{mp}), 3.48 (s, 2H, CH_2^{mp2}), 2.85 (br s, 2H, CH_2^{mp}), 2.64 (br s, 2H, CH_2^{mp}), 2.44−2.25 (m, 7H, H^{cy3} + H^{cy5} + CH_3^{mp}), 0.94 (d, 3H, ^3J = 6.9 Hz, H^{cy4}), 0.91 (d, 3H, ^3J = 6.9 Hz, $H^{cy4\prime}$). ^{13}C NMR (125 MHz, DMSO-d_6): 168.05 (CH, C^{13}), 156.74 (C_q, C^{13a}), 156.20 (CH, C^{15}), 146.36 (C_q, C^8), 145.38 (C_q, C^{4a}), 144.24 (C_q, C^{11a}), 140.63 (CH, C^{17}), 139.49 (C_q, C^{10a}), 130.04 (CH, C^{16} or C^{18}), 129.98 (CH, C^{16} or C^{18}), 129.40 (CH, C^3), 128.26 (CH, C^4), 124.24 (CH, C^2), 122.54 (CH, C^1), 121.63 (C_q, C^{6b}), 120.46 (CH, C^9), 116.05 (CH, C^7), 115.99 (C_q, C^{11b}), 112.86 (CH, C^{10}), 106.64 (C_q, C^{6a}), 98.79 (C_q, C^{cy1a}), 96.63 (C_q, C^{cy2a}), 79.66 (CH, C^{cy2}), 79.10 (CH, $C^{cy2\prime}$), 75.67 (CH, C^{cy1}), 75.45 (CH, $C^{cy1\prime}$), 54.8 (CH_2, CH_2^{mp}), 49.5 (CH_2, CH_2^{mp}), 46.0 (CH_3, CH_3^{mp}), 31.25 (C_q, C^{cy3}), 22.57 (CH_3, C^{cy4}), 22.27 (CH_3, $C^{cy4\prime}$), 18.99 (CH_3, C^{cy5}) ppm, C^6 not observed.

Physical Measurements. One-dimensional (1D) ^{1}H and ^{13}C NMR and two-dimensional (2D) ^{1}H−^{1}H COSY, ^{1}H−^{1}H TOCSY, ^{1}H−^{1}H ROESY or ^{1}H−^{1}H NOESY, ^{1}H−^{13}C HSQC, and ^{1}H−^{13}C HMBC NMR spectra were recorded on two Bruker Avance III

dx.doi.org/10.1021/ic500825j | Inorg. Chem. 2014, 53, 6934−6943

Scheme 1. Synthetic Pathways to Prepare the Isomeric Indoloquinoline-Piperazine Hybrids 7a, 7b, and 7c[a]

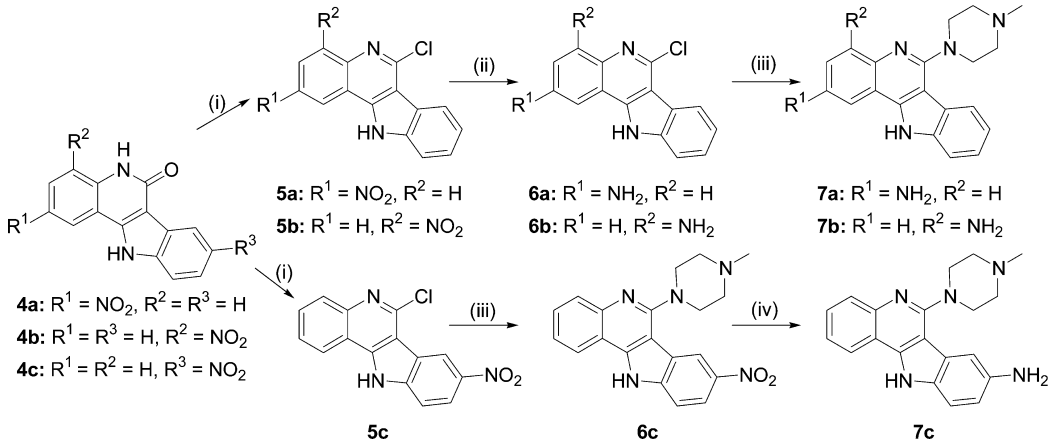

[a]Reagents and conditions: (i) $POCl_3$, Ar, 110 °C, 24 h; (ii) Fe (powder), AcOH, EtOH, 35 °C, 3−4 h, ultrasound bath; (iii) 1-methylpiperazine, Ar, 130 °C, 24 h; (iv) MeOH, 10% Pd/C, H_2, RT, 24 h.

spectrometers at 500.32 or 500.10 (^{1}H), and 125.82 or 125.76 (^{13}C) MHz, respectively, by using DMSO-d_6 as a solvent at room temperature and standard pulse programs. ^{1}H and ^{13}C shifts are quoted relative to the solvent residual signals. The atom numbering scheme used for NMR assignments is depicted in Supporting Information, Scheme S1. Electrospray ionization mass spectrometry (ESI-MS) was carried out with a Bruker Esquire 3000 instrument, and the samples were dissolved in methanol. Elemental analyses were performed at the Microanalytical Laboratory of the University of Vienna with a PerkinElmer 2400 CHN Elemental Analyzer (PerkinElmer, Waltham, MA). Hydrolysis studies were undertaken on a ThermoFisher Dionex UltiMate 3000 HPLC (Waltham, MA) device. The column compartment was kept at 298 K. A Hypersil Gold C18 Reversed phase Silica Column (250 × 4.6 mm, 5 μm particle size, ThermoFisher; Waltham, MA) equipped with a guard column was used. The complexes were dissolved in either pure deionized water or phosphate buffer at pH 7.40 so that the final concentrations were 100 mM or 75 μM, respectively. Samples were automatically injected into the HPLC, and separation of the hydrolysis products was achieved by applying gradient elution (5−80% or 10−50% acetonitrile in 15 mM aqueous formic acid). Detection and quantification of the peaks was conducted using the ThermoFisher Dionex DAD-3000RS UV detector (Waltham, MA) at a wavelength of 300 nm and the Chromeleon 7 software package (ThermoFisher Dionex, Sunnyvale, CA). In the case of [**2b**]Cl, further identification of the peaks was done by collecting the main fractions and analyzing them using a Bruker micrOTOF-Q2 ESI-MS instrument.

Crystallographic Structure Determination. X-ray diffraction measurements were performed on a Bruker X8 APEXII CCD diffractometer. Single crystals were positioned at 35, 40, and 35 mm from the detector, and 969, 790, and 2330 frames were measured, each for 60, 90, and 20 s over 1° scan width for [**1a**H]Cl_2·EtOH·$2H_2O$, [**2a**H]Cl_2·1.5^{i}PrOH·$0.5H_2O$, and [**2a**]Cl·0.5EtOH·H_2O, respectively. The data were processed using SAINT software.[48] Crystal data, data collection parameters, and structure refinement details are given in Table 1. The structures were solved by direct methods and refined by full-matrix least-squares techniques. Non-hydrogen atoms were refined with anisotropic displacement parameters. H atoms were inserted in calculated positions and refined with a riding model. The following computer programs and hardware were used: structure solution, *SHELXS-97*; structure refinement, *SHELXL-97*;[49] molecular diagrams, ORTEP.[50]

Cell Culture. Human SK-N-MC neuroepithelioma cells were obtained from the American Type Culture Collection (ATCC; Manassas, VA). The SK-N-MC cell type was grown as described previously.[51]

MTT Assay. The effect of complexes [**1a,b**]Cl−[**3a,b**]Cl on the cellular proliferation of SK-N-MC cells was examined using the 1-(4,5-dimethylthiazol-2-yl)-2,5-diphenyl-tetrazolium (MTT) assay by standard techniques.[52,53] Human SK-N-MC cells were chosen for these studies as the antiproliferative effect of metal complexes has been extensively examined in this cell type.[52−54] MTT reduction is proportional to viable cell counts using SK-N-MC cells.[51] SK-N-MC cells were seeded at 1.5 × 10^4 cells/well in 96-well microtiter plates in a medium containing the compounds (0−50 μM) and human diferric transferrin (Tf) at 1.25 μM ([Fe] = 2.5 μM). Control samples contained Tf (1.25 μM) in the absence of the compounds. Notably, Tf is utilized as it is the physiological iron donor and is required for cellular proliferation.[51] It is essential to add to the media when assessing the antiproliferative activity of the ligands used as positive controls, namely, desferrioxamine (DFO), di-2-pyridylketone 4,4-dimethyl-3-thiosemicarbazone (Dp44mT), and Doxorubicin.[61] The cells were incubated at 37 °C for 72 h, after which 10 μL of MTT solution (stock solution: 5 mg/mL) was added to each well and incubated for 2 h at 37 °C. After cell solubilization using 100 μL of 10% SDS−50% isobutanol in 0.01 M HCl, the plates were read at 570 nm using a scanning multiwell spectrophotometer. The inhibitory concentration (IC_{50}) was defined as the concentration of the compound necessary to reduce the absorbance to 50% of the untreated control.

Statistical Analysis. Results are expressed as mean ± standard deviation (SD). Statistical comparisons were performed using Prism v6 (GraphPad Software, Inc., La Jolla, CA) implementing a one-way ANOVA with a Bonferroni posthoc test and were considered statistically significant when $p < 0.05$.

RESULTS AND DISCUSSION

These studies examined the effects of attachment of the piperazine heterocycle to the indoloquinoline scaffold and of varying the position of the same metal-binding site on the indoloquinoline backbone. This resulted in the generation of three different structural isomers of the indoloquinoline−piperazine hybrid. The effect of the metal-binding site position on the antiproliferative activity of the resultant ruthenium and osmium complexes [**1a,b**]Cl−[**3a,b**]Cl was examined. The ruthenium and osmium complexes were assembled *in situ* by reacting the corresponding indoloquinoline−piperazine hybrid precursors **7a−c** containing an amino group at the 2-, 4-, or 8-position of the indoloquinoline scaffold with 2-pyridinecarboxaldehyde.

Attempts to isolate the pure indoloquinoline−piperazine hybrids in the absence of ruthenium(II) or osmium(II) failed. Thus, the compounds L^{1-3} and their resultant ruthenium and

dx.doi.org/10.1021/ic500825j | Inorg. Chem. 2014, 53, 6934−6943

osmium complexes [**1a**,**b**]Cl−[**3a**,**b**]Cl were formed in a single reaction mixture *in situ*. This suggests that the indoloquinoline−piperazine hybrids were stabilized through their coordination with the ruthenium(II)- or osmium(II)-arene moieties. The combination of the indoloquinoline and piperazine substructures and the introduction of amino groups at the three different positions were accomplished as shown in Scheme 1.

The synthesis of 2-amino-6-chloroindolo[3,2-*c*]quinoline **6a** was performed as described previously.[29] Briefly, 5-nitroisatin and 2-aminobenzylamine were reacted in glacial acetic acid in a manner similar to the unsubstituted isatin.[55] The resulting 2-nitroindolo[3,2-*c*]quinoline-6-one **4a** was chlorinated using $POCl_3$ to give **5a**, again under conditions similar to those applied for the synthesis of the unsubstituted congener.[56] Reduction of the nitro group was carried out using an adaption[29] of the procedure published by Gamble et al. to afford **6a**.[57] 7-Nitroisatin was easily obtained by adaption of the procedure used for the synthesis of 2-nitroaniline (see Supporting Information for detail).[58] The 4-amino isomer **6b** was prepared by following the same synthetic route used for the synthesis of **6a**. Application of the same synthetic scheme failed to yield **6c** in acceptable yield and purity. However, starting from isatin and 2-amino-5-nitrobenzylamine, obtained by neutralization of its hydrochloride salt[46] with aqueous ammonia, resulted in the synthesis of 8-nitro-indolo[3,2-*c*]quinoline-6-one **4c** in low yield but acceptable purity. Subsequent chlorination of **4c** yielded 6-chloro-8-nitro-indolo-[3,2-*c*]quinoline **5c**. In the final step, the imidoyl chloride **6a** or **6b** was reacted with 1-methylpiperazine, yielding the corresponding 2- or 4-amino-6-(4-methylpiperazin-1-yl)-indolo[3,2-*c*]quinoline **7a** or **7b**, respectively. To obtain **7c**, compound **5c** was allowed to react with 1-methylpiperazine to yield **6c**, followed by the reduction of the nitro group at position 8 by using H_2 and Pd/C as shown in Scheme 1.

Further condensation reactions of the indoloquinoline−piperazine hybrids **7a**−**7c** with 2-pyridinecarboxaldehyde in the presence of $[RuCl(\mu\text{-}Cl)(\eta^6\text{-}p\text{-cymene})]_2$ or $[OsCl(\mu\text{-}Cl)(\eta^6\text{-}p\text{-cymene})]_2$ afforded the chelating bidentate ligands isolated as metal-arene complexes [**1a**,**b**]Cl−[**3a**,**b**]Cl shown in Chart 1. Note that, because of the enhanced aqueous solubility of two series of isomeric complexes [**1a**]Cl−[**3a**]Cl and [**1b**]Cl−[**3b**]Cl, the purification method had to be modified. Microcrystalline osmium complexes [**1b**]Cl−[**3b**]Cl as well as ruthenium complex [**3a**]Cl could be obtained with high purity by dropwise addition of the reaction mixture to large amounts of diethyl ether. Prior drying of diethyl ether over Na_2SO_4 was required to avoid the formation of a sticky oil. In the case of the ruthenium complexes [**1a**]Cl and [**2a**]Cl, this procedure led to the coprecipitation of small amounts of side products. Pure compounds, obtained when condensation reactions in the presence of $[RuCl(\mu\text{-}Cl)(\eta^6\text{-}p\text{-cymene})]_2$ were carried out in water, were isolated from concentrated aqueous solutions. All complexes were characterized by elemental analysis, ESI mass spectrometry, and spectroscopic methods. The compounds are moderately hygroscopic; water, which had to be included in the elemental formulas, is a property common to nearly all metal complexes with modified indoloquinolines reported so far.[23,27−29] The *in situ* formation of the ligands during the complex syntheses of [**1a**]Cl−[**3a**]Cl and [**1b**]Cl−[**3b**]Cl was confirmed by the presence of strong peaks at *m*/*z* 691 and *m*/*z* 781, respectively, attributed to the $[M-Cl]^+$ ion.

The 1D and 2D NMR spectra showed chemical shifts typical for this class of compounds,[23,27−29] in particular, the rather upfield-shifted resonances for carbon atom C^{6a} (for the atom numbering scheme used for the assignment of resonances see Supporting Information, Scheme S1) at approximately 106−107 ppm. Although a weak resonance for quaternary carbon atom C^6 could be seen in complexes [**1a**]Cl and [**1b**]Cl, this was not detected in the remaining four metal complexes. Note that such isolated quaternary carbons are generally hard to detect, as they do not display in standard 2D $^1H-^{13}C$ NMR experiments like HSQC or HMBC. They also have much longer relaxation times compared to those with protons in close proximity, leading to weakening or even suppression of the signal in standard ^{13}C NMR experiments. However, the shift of approximately 158.5 ppm for C^6 in the ^{13}C NMR spectra of [**1a**]Cl and [**1b**]Cl is in good agreement with that featured by related indoloquinolines, in which the piperazine ring is substituted by an ethylenediamine moiety.[23] Due to the presence of the stereogenic metal center, the adjacent cymene protons showed diastereotopic splitting, leading to four distinct signals for the aromatic protons. In addition, two resonances were observed for the protons of the isopropyl groups. This pattern is typical for racemic ruthenium-arene complexes, in which bulky ligand(s) hinder the free rotation of the arene.[59,60] Furthermore, because of the flexibility of the piperazine ring, the unequivocal assignment of the resonances observed was not possible. Therefore, the CH_2 resonances present as broad singlets were assigned as CH_2^{mp}.

Stability in DMSO, Solubility in Phosphate Buffer, and Hydrolytic Behavior. Complexes [**3a**]Cl and [**3b**]Cl remain intact when dissolved in DMSO. ESI mass spectra of solutions of [**3a**]Cl and [**3b**]Cl in DMSO diluted with methanol 1:100 showed intense peaks with *m*/*z* 691 and 781, respectively, attributed to $[M-Cl]^+$ ions (Supporting Information, Figures S1 and S2). Basically, the same mass spectra were obtained for 19 h old DMSO solutions of [**3a**]Cl and [**3b**]Cl after dilution with methanol. Hence, the dissolution of these complexes in DMSO does not lead to an appreciable replacement of Cl^- with DMSO.

The complexes presented herein are readily soluble in aqueous media. The solubility of all six complexes [**1a**,**b**]Cl−[**3a**,**b**]Cl in phosphate buffer (20 mM NaH_2PO_4/Na_2HPO_4 buffer at pH 7.40) exceeded 7 mM, regardless of the position of the coordinating moiety.

The stability of [**2a**]Cl and [**2b**]Cl in aqueous media over 24 h was further investigated by HPLC (Figure 2). Their stability in deionized water (Supporting Information, Figure S3) is very similar to that in buffered solution at physiological pH (Supporting Information, Figure S4; 20 mM NaH_2PO_4/Na_2HPO_4 buffer at pH 7.40). As can be seen from Supporting Information, Figure S4, greater than 90% of both the ruthenium complex [**2a**]Cl as well as its osmium counterpart [**2b**]Cl were hydrolyzed after 24 h, without any noticeable difference in the hydrolysis rate. A closer assessment revealed that [**2b**]Cl gave almost exclusively one hydrolysis product. However, in the case of its ruthenium analogue [**2a**]Cl, a second, minor species appeared between the parent peak and the less-retained hydrolysis peak (see Supporting Information, Figures S3 and S4 for chromatograms). Attempts to establish the nature of the predominant hydrolysis reactions were then performed. The fractions containing the two peaks from the hydrolysis of [**2a**]Cl were collected and subjected to high-resolution ESI mass spectrometry. The most abundant mass at *m*/*z* 373.1397

dx.doi.org/10.1021/ic500825j | *Inorg. Chem.* 2014, 53, 6934−6943

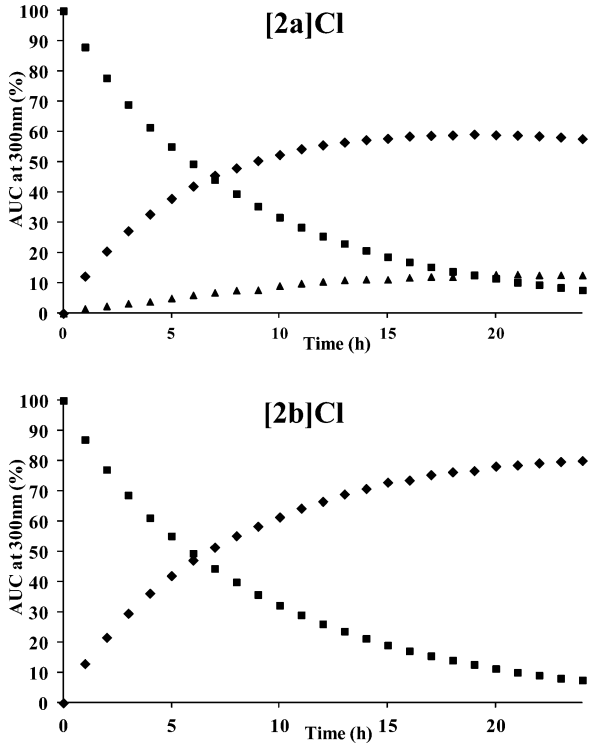

Figure 2. Hydrolysis curves of 75 μM solutions of complex [**2a**]Cl (top) and [**2b**]Cl (bottom) in 20 mM phosphate buffer at pH 7.40. For both complexes, the chlorido species concentration (■) steadily decreases with an estimated half-lifetime of approximately 6 h. In the case of [**2b**]Cl, only one hydrolysis product is formed (◆), whereas in the case of [**2a**]Cl, a third species (▲) is formed to a minor extent, exhibiting an area under curve (AUC) of approximately 12% compared to the staring material after 24 h. Data were recorded every hour over 24 h using HPLC with UV detection at 300 nm (see Experimental Section for details). Quantification was done by normalizing the AUC to the AUC at 0 h.

could be attributed to the doubly charged fragment $[M-2Cl]^{2+}$, whereas the second peak at m/z 736.2786 was assigned to the hydroxido species $[M-2Cl+OH]^{+}$, clearly stemming from hydrolysis of the chlorido ligand. The fraction containing the peak with the longer retention time showed mainly the parent ion $[M-Cl]^{+}$ at m/z 781.2442, and, to a lesser extent, the doubly charged $[M-2Cl]^{2+}$ ion. These data suggest that the *N*,*N*-bound ligand remained coordinated to the metal center, showing no signs of ligand cleavage.

X-ray Crystallography. The results of the X-ray diffraction studies of $[(\eta^6\text{-}p\text{-cymene})Ru(HL^1)Cl]Cl_2\cdot EtOH\cdot 2H_2O$ ([**1a**H]$Cl_2\cdot$EtOH$\cdot 2H_2O$), $[(\eta^6\text{-}p\text{-cymene})Ru(HL^2)Cl]Cl_2\cdot 1.5^{i}PrOH\cdot 0.5H_2O$ ([**2a**H]$Cl_2\cdot 1.5i$-PrOH$\cdot 0.5H_2O$), and $[(\eta^6\text{-}p\text{-cymene})Ru(L^2)Cl]Cl\cdot 0.5EtOH\cdot H_2O$ ([**2a**]Cl$\cdot 0.5$EtOH$\cdot H_2O$) are shown in Figures 3−5, respectively. The complexes [**1a**H]$Cl_2\cdot$EtOH$\cdot 2H_2O$, [**2a**H]$Cl_2\cdot 1.5^{i}$PrOH$\cdot 0.5H_2O$, and [**2a**]Cl$\cdot 0.5$EtOH$\cdot H_2O$ crystallized in the monoclinic centrosymmetric space groups $P2_1/n$, $P2_1/c$ and noncentrosymmetric *Pc*, respectively. All complexes studied contain a stereogenic ruthenium center and crystallize as racemates. The asymmetric units of the first two compounds consist of a complex dication, two chlorides as counteranions, and cocrystallized solvent, while that of the third complex consists of a complex monocation, one chloride as counteranion, and cocrystallized solvent molecules.

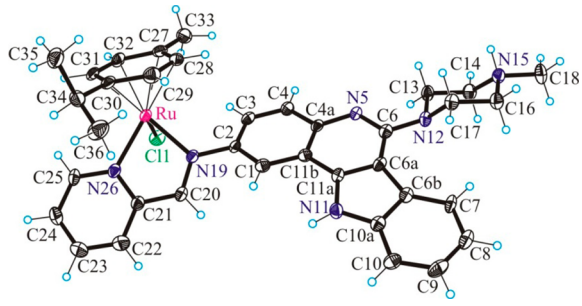

Figure 3. ORTEP view of the cation $[(\eta^6\text{-}p\text{-cymene})Ru(HL^1)Cl]^{2+}$ in [**1a**H]$Cl_2\cdot$EtOH$\cdot 2H_2O$ with thermal displacement parameters drawn at the 50% probability level. Selected bond distances (Å) and angles (deg): Ru−N19 2.091(3), Ru−N26 2.081(4), Ru−Cl1 2.387(1), Ru−C_{arene}(av) 2.20(1), N5−C6 1.318(5), C6−N12 1.402(6); N19−Ru−N26 77.18, $\Theta_{C1-C2-N19-C20}$ −33.6(6), $\Theta_{N19-C20-C21-N26}$ 0.6(6).

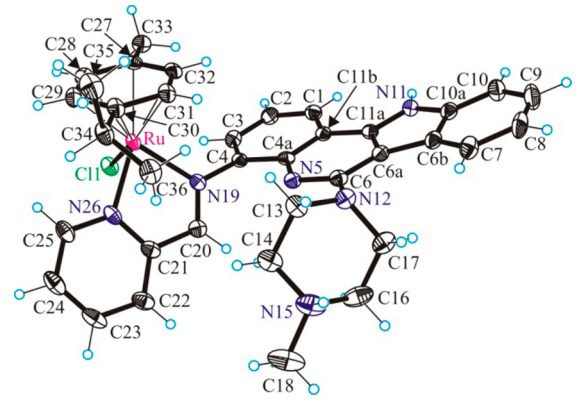

Figure 4. ORTEP view of the cation $[(\eta^6\text{-}p\text{-cymene})Ru(HL^2)Cl]^{2+}$ in [**2a**H]$Cl_2\cdot 1.5^{i}$PrOH$\cdot 0.5H_2O$ with thermal displacement parameters drawn at the 40% probability level. Selected bond distances (Å) and angles (deg): Ru−N19 2.073(4), Ru−N26 2.085(4), Ru−Cl1 2.382(1), Ru−C_{arene}(av) 2.194(7), N5−C6 1.314(5), C6−N12 1.400(6); N19−Ru−N26 77.1(1), $\Theta_{C4a-C4-N19-C20}$ −60.4(5), $\Theta_{N19-C20-C21-N26}$ 1.0(5).

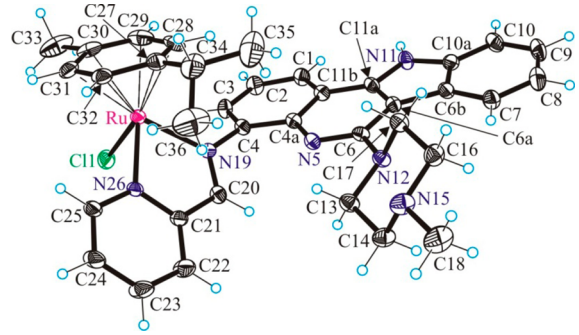

Figure 5. ORTEP view of the cation $[(\eta^6\text{-}p\text{-cymene})Ru(L^2)Cl]^{+}$ in [**2a**]Cl$\cdot 0.5$EtOH$\cdot H_2O$ with thermal displacement parameters drawn at the 50% probability level. Selected bond distances (Å) and angles (deg): Ru−N19 2.096(2), Ru−N26 2.073(2), Ru−Cl1 2.3838(8), Ru−C_{arene}(av) 2.20(2), N5−C6 1.311(4), C6−N12 1.393(4); N19−Ru−N26 76.4(1), $\Theta_{C4a-C4-N19-C20}$ −51.2(4), $\Theta_{N19-C20-C21-N26}$ 1.7(4).

All three complexes have a typical "three-leg piano-stool" geometry of ruthenium(II)-arene complexes, with a η^6 π-bound *p*-cymene ring forming the seat and three other donor atoms (two nitrogens, N19 and N26, of indolo[3,2-*c*]quinoline and one chloride ligand) as the legs of the stool. In the first two

dx.doi.org/10.1021/ic500825j | *Inorg. Chem.* 2014, 53, 6934−6943

complexes, the ligand is protonated at N15, while in the last complex the ligand is neutral. The protonation is corroborated by the presence of hydrogen-bonding interactions of the type N15−H···Cl2^{ii} in [**1a**H]Cl_2 and N15−H···Cl3^{ii} and N15−H···Cl3^{iii} in [**2a**H]Cl_2. Hydrogen-bonding interactions of the type N−H···Cl, in which N11 acts as a proton donor and Cl^- as proton acceptor, are evident in all three crystal structures (for hydrogen bond geometries see Supporting Information, Table S1).

The piperazine ring in all three compounds adopts a chair conformation. The conformations of the neutral ligand L^2 in the cation $[(\eta^6\text{-}p\text{-cymene})Ru(L^2)Cl]^+$ and the protonated ligand $(HL^2)^+$ in $[(\eta^6\text{-}p\text{-cymene})Ru(HL^2)Cl]^{2+}$ are similar, as can be seen in Supporting Information, Figure S5 showing a model fitting plot for the two cations. Of note is the slightly different orientation of the metal-binding site in both cations, which can be described by the torsional angle $\Theta_{C4a-C4-N19-C20}$ that differs by 9.2° and by the more divergent orientation of the six-membered piperazine heterocycle in two compounds. In addition, protonation of the piperazine ring led to counter-clockwise rotation of the *p*-cymene ring by approximately 39° around *p*-cymene ring centroid-Ru vector in $[(\eta^6\text{-}p\text{-cymene})\text{-}Ru(L^2)Cl]^+$ (see Supporting Information, Figure S5).

Anti-Proliferative Activity Against Tumor Cells. The ability of the isomeric ruthenium- and osmium-arene complexes of the indoloquinoline−piperazine hybrid ligands to inhibit cellular proliferation was examined using human SK-N-MC neuroepithelioma cells. These cells were utilized since the ability of other metal complexes to affect their growth is well-characterized.[52−54] The novel complexes [**1a**,**b**]Cl−[**3a**,**b**]Cl were compared to a number of relevant positive controls that form metal complexes and have been extensively examined in this cell type. These included: (1) DFO, which is used clinically for the treatment of iron overload disease;[61] (2) Dp44mT, an iron chelator that demonstrates potent antitumor activity *in vitro*[53] and *in vivo*;[62] and (3) doxorubicin (DOX), which is a clinically used cytotoxic agent.[63,64]

As previously observed,[53] the control chelator Dp44mT demonstrated the most potent antiproliferative effects of all the agents examined (IC_{50}: 0.004 ± 0.003 μM; Table 2). In contrast, the other positive controls, DOX (IC_{50}: 0.15 ± 0.05 μM; Table 2) and DFO (IC_{50}: 9.83 ± 0.39 μM; Table 2), demonstrated moderate and poor ability to inhibit the growth of SK-N-MC cells, respectively.

Table 2. IC_{50} (μM) Values of [1a,b]Cl−[3a,b]Cl at Inhibiting the Growth of SK-N-MC Neuroepithelioma Cells As Determined by the MTT Assay

compound	IC_{50} (μM)[a]
DFO	9.83 ± 0.39
Dp44mT	0.004 ± 0.003
DOX	0.15 ± 0.05
[**1a**]Cl	39.81 ± 2.07
[**1b**]Cl	>50
[**2a**]Cl	18.41 ± 2.22
[**2b**]Cl	19.40 ± 1.28
[**3a**]Cl	>50
[**3b**]Cl	41.24 ± 2.37

[a]Assays conducted for 72 h. Results are mean ± SD (three experiments).

Of the ruthenium and osmium complexes that contain the metal-binding site at the position 4 of the indoloquinoline scaffold, complexes [**2a**]Cl (IC_{50}: 18.41 ± 2.22 μM; Table 2) and [**2b**]Cl (IC_{50}: 19.40 ± 1.28 μM; Table 2) demonstrated significantly ($p < 0.001$) greater antiproliferative effects than the other ruthenium and osmium complexes examined. However, the anticancer activity of [**2a**]Cl and [**2b**]Cl was significantly ($p < 0.001$) less potent than that of the positive controls, Dp44mT, DFO, or DOX. Although [**1a**]Cl and [**3b**]Cl demonstrated comparable IC_{50} values (39.81 ± 2.07 μM cf. 41.24 ± 2.37 μM, respectively), both [**1b**]Cl and [**3a**]Cl did not exhibit marked antiproliferative effects with IC_{50} values > 50 μM.

Interestingly, these data illustrated the important role of the position of the metal-binding site on the anticancer activity of these isomeric Ru- and Os-arene complexes with indoloquinoline−piperazine conjugates. Those complexes containing the metal-binding site located at the 4 position of the indoloquinoline scaffold, namely, ([**2a**]Cl and [**2b**]Cl) demonstrated the most potent antiproliferative effects. In contrast, the Ru and Os complexes that contained the metal-binding site located at the 2 or 8 positions exhibited significantly ($p < 0.001$) decreased anticancer effects. Importantly, the position of the metal-binding site played a more critical role than the identity of the complexed metal in the antiproliferative activity of these agents.

CONCLUSIONS

In this study, the two bioactive substructures, namely, that of the indoloquinoline backbone with a piperazine heterocycle, were combined to improve the aqueous solubility of the resulting products, which can act as ligands to form ruthenium and osmium complexes. In addition to incorporating the piperazine heterocycle, these studies also examined the possibility of varying the position of the same metal-binding site on the indoloquinoline backbone. This resulted in the generation of three different structural isomers of the indoloquinoline−piperazine hybrid ligands. The effect of this structural combination on the antiproliferative activity of the resulting ruthenium- and osmium-arene complexes [**1a**,**b**]Cl−[**3a**,**b**]Cl was studied.

The data obtained illustrate the important role of the position of the metal-binding site on the anticancer activity of these isomeric ruthenium- and osmium-arene complexes with indoloquinoline−piperazine hybrids. Whereas the position of the metal-binding site does not have a marked effect on the solubility of [**1a**,**b**]Cl−[**3a**,**b**]Cl in phosphate buffer, the complexes containing the metal-binding site located at the position 4 of the indoloquinoline scaffold ([**2a**]Cl and [**2b**]Cl) demonstrated the most potent antiproliferative effects. In contrast, the ruthenium and osmium complexes that contain the metal-binding site located at the 2 or 8 position exhibited decreased antiproliferative activity. Importantly, the position of the metal-binding site played a more critical role than the identity of the complexed metal in the antiproliferative efficacy of these agents. These data highlight important structure−activity relationships that can be further utilized in the design of more potent anticancer ruthenium and osmium complexes based on indoloquinoline−piperazine hybrids.

ASSOCIATED CONTENT

Supporting Information

Synthesis of 7-nitroisatin, 2-amino-6-(4-methylpiperazin-1-yl)-indolo[3,2-*c*]quinoline, 4-nitroindolo[3,2-*c*]quinolin-6-one, 6-

dx.doi.org/10.1021/ic500825j | Inorg. Chem. 2014, 53, 6934−6943

chloro-4-nitroindolo[3,2-*c*]quinoline, 4-amino-6-chloroindolo-[3,2-*c*]quinoline, 4-amino-6-(4-methylpiperazin-1-yl)indolo-[3,2-*c*]quinoline, 8-nitroindolo[3,2-*c*]quinolin-6-one, 6-chloro-8-nitroindolo[3,2-*c*]quinoline, 6-(4-methylpiperazin-1-yl)-8-nitroindolo[3,2-*c*]quinoline, and 8-amino-6-(4-methylpiperazin-1-yl)indolo[3,2-*c*]quinoline, numbering scheme used for the assignment of NMR resonances (Scheme S1); ESI mass spectra of solutions of [**3a**]Cl and [**3b**]Cl in DMSO diluted 1:100 with methanol (Figures S1 and S2); HPLC data showing hydrolysis of complexes [**2a**,**b**]Cl (Figures S3 and S4); model fitting plot for $[(\eta^6\text{-}p\text{-cymene})Ru(L^2)Cl]^+$ and $[(\eta^6\text{-}p\text{-cymene})Ru(HL^2)Cl]^{2+}$ (Figure S5). Table S1 containing H-bond geometries and crystallographic data in CIF format. This material is available free of charge via the Internet at http://pubs.acs.org.

AUTHOR INFORMATION

Corresponding Authors

*E-mail: vladimir.arion@univie.ac.at. (V.B.A.)
*E-mail: danutak@med.usyd.edu.au. (D.S.K.)
*E-mail: d.richardson@med.usyd.edu.au. (D.R.R.)

Notes

The authors declare no competing financial interest.

ACKNOWLEDGMENTS

We thank Prof. Dr. M. Galanski for recording the 2D NMR spectra of complexes [**1a**,**b**]Cl−[**3a**,**b**]Cl, A. Dobrov and Dr. N. Lloyd for ESI mass spectra measurements, and A. Roller for collection of the X-ray data. We are also indebted to the Austrian Science Fund (FWF) for financial support of Project No. P22339−N19. D.R.R. thanks the National Health and Medical Research Council of Australia for a Senior Principal Research Fellowship (1062607) and Project Grants (1060482 and 1021607). D.S.K. acknowledges the NHMRC for Project Grant 1048972 and also the Sydney Medical School Foundation of The University of Sydney for a Helen and Robert Ellis Fellowship.

REFERENCES

(1) Sava, G.; Jaouen, G.; Hillard, E. A.; Bergamo, A. *Dalton Trans.* **2012**, *41*, 8226−8234.
(2) Smith, G. S.; Therrien, B. *Dalton Trans.* **2011**, *40*, 10793−10800.
(3) Noffke, A. L.; Habtemariam, A.; Pizzaro, A. M.; Sadler, P. J. *Chem. Commun.* **2012**, *48*, 5219−5246.
(4) Ang, W. H.; Casini, A.; Sava, G.; Dyson, P. J. *J. Organomet. Chem.* **2011**, *696*, 989−998.
(5) Nazarov, A. A.; Hartinger, C. G.; Dyson, P. J. *J. Organomet. Chem.* **2014**, *751*, 251−260.
(6) Hartinger, C. G.; Metzler-Nolte, N.; Dyson, P. J. *Organometallics* **2012**, *31*, 5677−5685.
(7) Kilpin, K. J.; Dyson, P. J. *Chem. Sci.* **2013**, *4*, 1410−1419.
(8) Kandioller, W.; Kurzwernhart, A.; Hanif, M.; Meier, S. M.; Henke, H.; Keppler, B. K.; Hartinger, C. G. *J. Organomet. Chem.* **2011**, *696*, 999−1010.
(9) (a) Castonguay, A.; Doucet, C.; Maysinger, D. *J. Med. Chem.* **2012**, *55*, 8799−8806. (b) Savić, A.; Dulović, M.; Poljarević, J. M.; Misirlić-Denčić, S.; Jovanović, M.; Bogdanović, A.; Trajković, V.; Sabo, T. J.; Grgurić-Šipka, S.; Marković, I. *ChemMedChem* **2011**, *6*, 1884−1891. (c) Ruiz, J.; Rodríguez, V.; Cutillas, N.; Espinosa, A.; Hannon, M. J. *Inorg. Chem.* **2011**, *50*, 9164−9171.
(10) Zaharevitz, D. W.; Gussio, R.; Leost, M.; Senderowicz, A. M.; Lahusen, T.; Kunick, C.; Meijer, L.; Sausville, E. A. *Cancer Res.* **1999**, *59*, 2566−2569.
(11) Schulz, C.; Link, A.; Leost, M.; Zaharevitz, D. W.; Gussio, R.; Sausville, E. A.; Meijer, L.; Kunick, C. *J. Med. Chem.* **1999**, *42*, 2909−2919.
(12) Knockaert, M.; Wieking, K.; Schmitt, S.; Leost, M.; Grant, K. M.; Mottram, J. C.; Kunick, C.; Meijer, L. *J. Biol. Chem.* **2002**, *277*, 25493−25501.
(13) Tolle, N.; Kunick, C. *Curr. Top. Med. Chem.* **2011**, *11*, 1320−1332.
(14) Kunick, C.; Lauenroth, K.; Leost, M.; Meijer, L.; Lemcke, T. *Bioorg. Med. Chem. Lett.* **2004**, *14*, 413−416.
(15) Becker, A.; Kohfeld, S.; Lader, A.; Preu, L.; Pies, T.; Wieking, K.; Ferandin, Y.; Knockaert, M.; Meijer, L.; Kunick, C. *Eur. J. Med. Chem.* **2010**, *45*, 335−342.
(16) Dobrov, A.; Arion, V. B.; Kandler, N.; Ginzinger, W.; Jakupec, M. A.; Rufinska, A.; Graf von Keyserlingk, N.; Galanski, M.; Kowol, C.; Keppler, B. K. *Inorg. Chem.* **2006**, *45*, 1945−1950.
(17) Ginzinger, W.; Arion, V. B.; Giester, G.; Galanski, M.; Keppler, B. K. *Cent. Eur. J. Chem.* **2008**, *6*, 340−346.
(18) Schmid, W. F.; Zorbas-Seifried, S.; John, R. O.; Arion, V. B.; Jakupec, M. A.; Roller, A.; Galanski, M.; Chiorescu, I.; Zorbas, H.; Keppler, B. K. *Inorg. Chem.* **2007**, *46*, 3645−3656.
(19) Primik, M. F.; Mühlgassner, G.; Jakupec, M. A.; Zava, O.; Dyson, P. J.; Arion, V. B.; Keppler, B. K. *Inorg. Chem.* **2010**, *49*, 302−311.
(20) Schmid, W. F.; John, R. O.; Mühlgassner, G.; Heffeter, P.; Jakupec, M. A.; Galanski, M.; Berger, W.; Arion, V. B.; Keppler, B. K. *J. Med. Chem.* **2007**, *50*, 6343−6355.
(21) Schmid, W. F.; John, R. O.; Arion, V. B.; Jakupec, M. A.; Keppler, B. K. *Organometallics* **2007**, *26*, 6643−6652.
(22) Mühlgassner, G.; Bartel, C.; Schmid, W. F.; Jakupec, M. A.; Arion, V. B.; Keppler, B. K. *J. Inorg. Biochem.* **2012**, *116*, 180−187.
(23) Filak, L. K.; Mühlgassner, G.; Jakupec, M. A.; Heffeter, P.; Berger, W.; Arion, V. B.; Keppler, B. K. *J. Biol. Inorg. Chem.* **2010**, *15*, 903−918.
(24) Arion, V. B.; Dobrov, A.; Goeschl, S.; Jakupec, M. A.; Keppler, B. K.; Rapta, P. *Chem. Commun.* **2012**, *48*, 8559−8561.
(25) Primik, M. F.; Filak, L. K.; Arion, V. B. Metal-Based Indolobenzazepines and Indoloquinolines: From Moderate CDK Inhibitors to Potential Antitumor Drugs. In *Advances in Organometallic Chemistry and Catalysis: The Silver/Gold Jubilee International Conference on Organometallic Chemistry Celebratory Book,* 1st ed.; Pombeiro, A. J. L., Ed.; John Wiley & Sons: Hoboken, NJ, 2014, pp 605−617.
(26) Lavrado, J.; Moreira, R.; Paulo, A. *Curr. Med. Chem.* **2010**, *17*, 2348−2370.
(27) Filak, L. K.; Mühlgassner, G.; Bacher, F.; Roller, A.; Galanski, M.; Jakupec, M. A.; Keppler, B. K.; Arion, V. B. *Organometallics* **2011**, *30*, 273−283.
(28) Filak, L. K.; Göschl, S.; Hackl, S.; Jakupec, M. A.; Arion, V. B. *Inorg. Chim. Acta* **2012**, *393*, 252−260.
(29) Filak, L. K.; Göschl, S.; Heffeter, P.; Ghannadzadeh Samper, K.; Egger, A. E.; Jakupec, M. A.; Keppler, B. K.; Berger, W.; Arion, V. B. *Organometallics* **2013**, *32*, 903−914.
(30) (a) Ae, N.; Fujiwara, Y.; US 20110263847 A1, 2011. (b) Kakiya, Y.; Oda, M. WO 2005009999 A1, 2005. (c) Ochi, T.; Sakamoto, M.; Minamida, A.; Suzuki, K.; Ueda, T.; Une, T.; Toda, H.; Matsumoto, K.; Terauchi, Y. *Bioorg. Med. Chem. Lett.* **2005**, *15*, 1055−1059. (d) Chen, B. C.; Droghini, R.; Lajeunesse, J.; DiMarco, J. D.; Gallela, M.; Chidambaram, R. US 2005215795, 2005.
(31) Kharb, R.; Bansal, K.; Sharma, A. K. *Pharm. Chem. J.* **2012**, *4*, 2470−2488.
(32) Faist, J.; Seebacher, W.; Saf, R.; Brun, R.; Kaiser, M.; Weis, R. *Eur. J. Med. Chem.* **2012**, *47*, 510−519.
(33) Kulig, K.; Sapa, J.; Maciag, D.; Filipek, B.; Malawska, B. *Arch. Pharm. (Weinheim, Germany)* **2007**, *340*, 466−475.
(34) Nelson, J. M.; Chiller, T. M.; Powers, J. H.; Angulo, F. J. *Clin. Infect. Dis.* **2007**, *44*, 977−980.
(35) Burka, J. M.; Bower, K. S.; Vanroekel, R. C.; Stutzman, R. D.; Kuzmowych, C. P.; Howard, R. S. *Am. J. Ophthalmol.* **2005**, *140*, 83−87.

(36) Schiller, D. S.; Fung, H. B. *Clin. Ther.* **2007**, *29*, 1862−1886.
(37) Macías, B.; Villa, M. V.; Rubio, I.; Castiñeiras, A.; Borrás, J. *J. Inorg. Biochem.* **2001**, *84*, 163−170.
(38) Drevenšek, P.; Košmrlj, J.; Giester, G.; Skauge, T.; Sletten, E.; Sepčić, K.; Turel, I. *J. Inorg. Biochem.* **2006**, *100*, 1755−1763.
(39) Turel, I.; Kljun, J.; Perdih, F.; Morozova, E.; Bakulev, V.; Kasyanenko, N.; Byl, J. A. W.; Osheroff, N. *Inorg. Chem.* **2010**, *49*, 10750−10752.
(40) Tarushi, A.; Polatoglou, E.; Kljun, J.; Turel, I.; Psomas, G.; Kessissoglou, D. P. *Dalton Trans.* **2011**, *40*, 9461−9473.
(41) Zia-ur-Rehman; Muhammad, N.; Ali, S.; Butler, I. S.; Meetsma, A. *Inorg. Chim. Acta* **2011**, *376*, 381−388.
(42) Troshina, O. A.; Troshin, P. A.; Peregudov, A. S.; Kozlovski, V. I.; Lyubovskaya, R. N. *Chem.—Eur. J.* **2006**, *12*, 5569−5577.
(43) Antonello, C.; Uriarte, E.; Palumbo, M.; Valisena, S.; Parolin, C.; Palù, G. *Eur. J. Med. Chem.* **1993**, *28*, 291−296.
(44) Moore, T. W.; Sana, K.; Yan, D.; Thepchatri, P.; Ndungu, J. M.; Saindane, M. T.; Lockwood, M. A.; Natchus, M. G.; Liotta, D. C.; Plemper, R. K.; Snyder, J. P.; Sun, A. *Beilstein J. Org. Chem.* **2013**, *9*, 197−203.
(45) Wang, S.; Jia, X.-D.; Liu, M.-L.; Lu, Y.; Guo, H.-Y. *Bioorg. Med. Chem. Lett.* **2012**, *22*, 5971−5975.
(46) Giordani, A.; Mandelli, S.; Verpilio, I.; Zanzola, S.; Tarchino, F.; Caselli, G.; Piepoli, T.; Mazzari, S.; Macovec, F.; Rovati, L. C. WO 2008014822 A1, 2008.
(47) Perrin, D. D.; Armarego, W. L. F. *Purification of Laboratory Chemicals;* Pergamon Press: New York, 1988.
(48) *SAINT-Plus, Version 7.06a and APEX2;* Bruker-Nonius AXS, Inc.: Madison, WI, 2004.
(49) Sheldrick, G. M. *Acta Crystallogr.* **2008**, *A64*, 112−122.
(50) Burnett, M. N.; Johnson, G. K. *ORTEPIII;* Technical Report ORNL-6895 for Oak Ridge National Laboratory; Oak Ridge, TN, 1996.
(51) Richardson, D. R.; Tran, E. H.; Ponka, P. *Blood* **1995**, *86*, 4295−4306.
(52) Kalinowski, D. S.; Yu, Y.; Sharpe, P. C.; Islam, M.; Liao, Y.-T.; Lovejoy, D. B.; Kumar, N.; Bernhardt, P. V.; Richardson, D. R. *J. Med. Chem.* **2007**, *50*, 3716−3719.
(53) Richardson, D. R.; Sharpe, P. C.; Lovejoy, D. B.; Senaratne, D.; Kalinowski, D. S.; Islam, M.; Bernhardt, P. V. *J. Med. Chem.* **2006**, *49*, 6510−6521.
(54) Bernhardt, P. V.; Sharpe, P. C.; Islam, M.; Lovejoy, D. B.; Kalinowski, D. S.; Richardson, D. R. *J. Med. Chem.* **2009**, *52*, 407−415.
(55) Bergman, J.; Engqwist, R.; Ståhlhandske, C.; Wallberg, H. *Tetrahedron* **2003**, *59*, 1033−1048.
(56) Primik, M. F.; Göschl, S.; Jakupec, M. A.; Roller, A.; Keppler, B. K.; Arion, V. B. *Inorg. Chem.* **2010**, *49*, 11084−11095.
(57) Gamble, A. B.; Garner, J.; Gordon, C. P.; O'Conner, S. M. J.; Keller, P. A. *Synth. Commun.* **2007**, *37*, 2777−2786.
(58) Polychronopoulos, P.; Magiatis, P.; Scalsounis, A.-L.; Myrianthopoulos, V.; Mikros, E.; Tarricone, A.; Musacchio, A.; Roe, S. M.; Pearl, L.; Leost, M.; Greengard, P.; Meijer, L. *J. Med. Chem.* **2004**, *47*, 935−946.
(59) Van Rijt, S. H.; Hebden, A. J.; Amaresekera, T.; Deeth, R. J.; Clarkson, G. J.; Parsons, S.; McGowan, P. C.; Sadler, P. J. *J. Med. Chem.* **2009**, *52*, 7753−7764.
(60) Meier, S. M.; Hanif, M.; Adhireksan, Z.; Pichler, V.; Novak, M.; Jirkovsky, E.; Jakupec, M. A.; Arion, V. B.; Davey, C. A.; Keppler, B. K.; Hartinger, C. G. *Chem. Sci.* **2013**, *4*, 1837−1846.
(61) Kalinowski, D. S.; Richardson, D. R. *Pharmacol. Rev.* **2005**, *57*, 547−583.
(62) Whitnall, M.; Howard, J.; Ponka, P.; Richardson, D. R. *Proc. Natl. Acad. Sci. U. S. A.* **2006**, *103*, 14901−14906.
(63) Tacar, O.; Sriamornsak, P.; Dass, C. R. *J. Pharm. Pharmacol.* **2013**, *65*, 157−170.
(64) Merlot, A. M.; Kalinowski, D. S.; Richardson, D. R. *Antioxid. Redox Signaling* **2013**, *18*, 973−1006.